Syngas Production from Protective Face Masks through Pyrolysis/Steam Gasification

energies

MDPI

Article

Syngas Production from Protective Face Masks through Pyrolysis/Steam Gasification

Ieva Kiminaitė [1], Judith González-Arias [2], Nerijus Striūgas [1], Justas Eimontas [1,*] and Martin Seemann [2]

[1] Laboratory of Combustion Processes, Lithuanian Energy Institute, Breslaujos str. 3, LT-44403 Kaunas, Lithuania
[2] Department of Space, Earth and Environment, Chalmers University of Technology, 412 96 Göteborg, Sweden
* Correspondence: justas.eimontas@lei.lt; Tel.: +370-37401976

Abstract: The COVID-19 pandemic has caused a heavy expansion of plastic pollution due to the extensive use of personal protective equipment (PPE) worldwide. To avoid problems related to the entrance of these wastes into the environment, proper management of the disposal is required. Here, the steam gasification/pyrolysis technique offers a reliable solution for the utilization of such wastes via chemical recycling into value-added products. The aim was to estimate the effect of thermo-chemical conversion temperature and steam-to-carbon ratio on the distribution of gaseous products obtained during non-catalytic steam gasification of 3-ply face masks and KN95 respirators in a fluidized bed reactor. Experimental results have revealed that the process temperature has a major influence on the composition of gases evolved. The production of syngas was significantly induced by temperature elevation from 700 °C to 800 °C. The highest molar concentration of H_2 gases synthesized from both types of face masks was estimated at 800 °C with the steam-to-carbon ratio varying from 0 to 2. A similar trend of production was also determined for CO gases. Therefore, investigated thermochemical conversion process is a feasible route for the conversion of used face masks to valuable a product such as syngas.

Keywords: personal protective equipment; steam gasification; pyrolysis; syngas production; fluidized bed reactor

Citation: Kiminaitė, I.; González-Arias, J.; Striūgas, N.; Eimontas, J.; Seemann, M. Syngas Production from Protective Face Masks through Pyrolysis/Steam Gasification. *Energies* **2023**, *16*, 5417. https://doi.org/10.3390/en16145417

Academic Editor: Gartzen Lopez

Received: 9 June 2023
Revised: 7 July 2023
Accepted: 13 July 2023
Published: 17 July 2023

1. Introduction

The COVID-19 pandemic officially declared by WHO on 11 March 2020 [1] has caused significant challenges to the health system together with numerous social, economic, and environmental concerns [2]. The typical way the highly contagious virus spreads is through airborne particles and droplets that are released when an infected person talks, sneezes, or coughs [3]. Thus, as an effective tool for disease prevention and control, disposable protective face masks were used on a large scale. Y. Peng et al. [4] have estimated that from the beginning of the pandemic till August 20, 8.4 ± 1.4 million tons of mismanaged plastic waste were generated globally, with around 7.6% contribution of personal protective equipment (PPE). According to the WHO data, approximately 87,000 tonnes of PPE, including face masks, gloves, protective clothing, and so on, were purchased and used until November 2021, with the majority of it turning out to be waste [5]. Since the end of the COVID-19 pandemic is in sight, the use of PPE has decreased compared to the amount of PPE employed at the peak periods of the pandemic, although it remains highly demanded in the healthcare sector in order to protect both healthcare personnel and patients from different infectious diseases [6]. Therefore, the generation of these wastes persists to date.

The management of PPE waste should be achieved in several stages. Health and environmental authorities have highlighted that protective masks used by infected patients and medical personnel must be considered bio-hazardous waste and combusted to avoid their accumulation together with sterilization in advance [7]. Due to the occurrence of errors in handling these abundant wastes, protective face masks as a prevention tool

for COVID-19 infection have substantially contributed to plastic pollution enlargement. Surveys have revealed that disposed personal protective equipment pollutes both aquatic and terrestrial environments causing direct damage to living organisms by entrapment or ingestion [8] of such wastes along with a micro-plastic pollution threat in aqueous and soil environments [9], which is harmful to the health of both humans and animals. Moreover, there are severe biological hazards when such medical wastes enter the environment—living organisms may be infected by contact with microorganisms remaining on used masks [10]. Consequently, proper management and reasonable utilization techniques are required to reduce the negative impacts of the disposed biomedical wastes on the environment and living organisms.

Highly demanded protective face masks are made of different plastic materials such as polypropylene, polyethylene terephthalate, polyvinyl chloride, polystyrene, polyethylene, and metallic parts. Therefore, recycling these wastes using mechanical means is barely conceivable due to the relatively complicated separation of the components [11]. Thus, thermal or thermochemical treatment of these disposals is a preferable solution under present conditions. The incineration of PPE wastes is a controversial pathway where scientific research has revealed that during the combustion of plastic materials, highly toxic pollutants such as polycyclic aromatic hydrocarbons are released into the air, which are carcinogens and negatively affect the human reproduction system [12], making them significant concerns in the context of the 22nd century. Consequently, the utilization of disposed PPE through thermochemical conversion becomes the most reliable solution.

Possible thermochemical conversion techniques of COVID-19 pandemic-related medical wastes were thoroughly reviewed by C. H. Purnomo et al. [13]. They indicated that pyrolysis and gasification are advantageous due to high energy conversion efficiency and minor environmental impacts. Production of valuable gases and oils from plastic wastes, including surgical face masks, can be implemented through the pyrolysis process, depending on the conditions of the process. The pyrolysis of a feedstock conversion to gaseous or liquid products is performed by the thermal degradation of a feedstock in the inert ambient by applying a sufficiently high heating rate in a range of 1–100 °C/s [14] and at a pyrolysis temperature which is higher than 500 °C [15]. Although, according to the previous research, the primary catalyst (mostly ZSM-5, HZSM-5, Al_2O_3, FCC, natural zeolite or Red Mud, which can additionally be doped with Ni-, Zn-, Mo-, and Co-) is generally employed to achieve the formation of low molecular weight gaseous products such as syngas [16]. S. Jung et al. [11] have revealed that utilization of 5 wt.% Ni/SiO_2 catalyst during the pyrolysis of protective face mask waste favors hydrogen and methane gas formation under N_2 ambient with the H_2 and CH_4 final concentrations of 55.1 and 18.2 mol%, respectively. In terms of gasification, in contrast to pyrolysis, an oxidizing agent, namely steam, air, CO_2, or O_2, is employed to chemically recycle different wastes into products of added value, with the main focus being on the gaseous ones [17]. A. Farooq et al. [18] investigated the thermochemical conversion of KF94 face masks via catalytic air and steam gasification. They declared that the highest concentration of hydrogen gases, equal to 45%, was detected with steam as the gasification agent by employing a Ni/m-ZSM-5(30) catalyst with 25% impregnated Ni. Comparable results were obtained by J. Nam et al. [19], who published that KF94 masks can be converted to hydrogen with a final concentration of almost 40% in product gas via steam gasification with activated carbon used to facilitate tar cracking (the estimated proportion of tars was 9–11% in the analyzed cases). Thus, previous investigations have confirmed that catalytic pyrolysis and steam gasification are proven tools for biomedical waste management over chemical recycling. Nevertheless, the use of catalysts in such thermochemical conversion processes is controversial regarding the sustainability aspect due to the relatively short lifetime of the catalysts exploited [20]. Deactivation of the catalyst occurs due to coking; thus, it should be frequently regenerated by applying oxidation, which affects the structure of the catalyst and the catalytic activity after repeating regeneration several times (depending on the type of catalyst) [21]. Therefore, to avoid the accumulation of additional wastes during the process, it is necessary to

evaluate the possibilities of thermochemical conversion of disposable face masks without catalyst material.

The novelty of the present research lies in the conditions and conversion type selected for the thermochemical processing of face mask pellets, which is a non-catalytic pyrolysis and steam gasification in a fluidized bed reactor. The aim was to analyze how the composition of product gases, along with the formation of char and tars, depends on the temperature and steam-to-carbon ratio applied during the pyrolysis and steam gasification of 3-ply and KN95 face masks.

2. Materials and Methods

2.1. Materials

Two types of disposable protective face masks were analyzed in this research—3-ply surgical face masks (3PFM) and respirators (KN95). It is known that 3PFM primarily consists of 3 filtering layers of non-woven fabric made of polypropylene. Whereas the KN95 masks contain from 3 to 5 layers of fabric, of which 2 are for filtration purposes made of polypropylene as well and a couple of structure support layers made of non-woven cotton. Masks also contain aluminum nose clips and ear loops comprised of polyester and spandex yarns.

To conduct gasification experiments in the fluidized bed reactor, used face masks were first shredded using a Filamaker Textile shredder with 15 mm blades and a 0.55 kW electric motor and pelletized afterward. Shredded feedstocks were granulated with a small capacity (5.5 kW) granulator to pellets of 8 mm diameter, as presented in Figure 1. Prepared pellets were first characterized by an ultimate analysis, determining the ash content as well. The Thermo Flash 2000 Elemental Analyzer was employed to implement the ultimate analysis experiments based on the ISO 17247:2020 international standard. The elemental composition data of the analyzed feedstocks used to determine steam-to-carbon values are displayed in Figure 1.

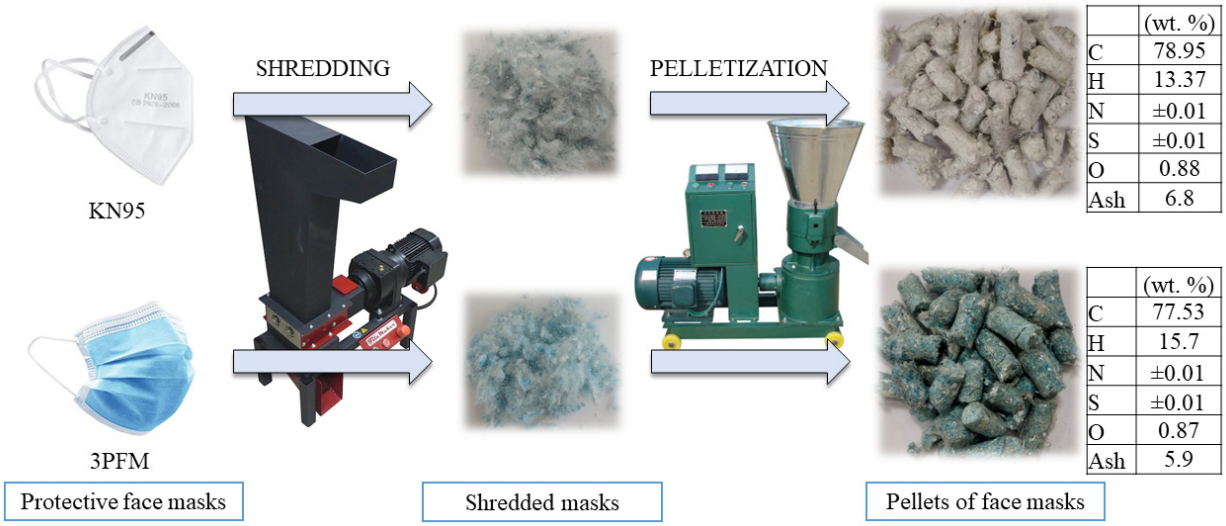

Figure 1. Schematic illustration of the preparation of pellets from used face masks.

2.2. Thermogravimetric Analysis

Thermal analysis of protective face masks was conducted by implementing a NETZSCH STA 449 F3 Jupiter analyzer (equipment sourced from NETZSCH, Selb, Germany). Samples of 10 ± 2 mg were placed in Al_2O_3 crucibles and heated from 50 to 900 °C temperature at a 20 °C/min heating rate under controlled conditions of the environment. Experiments were conducted in two atmospheres of different inertness. The thermal degradation characteristics of the shredded face masks were determined by conducting pyrolysis in the inert ambient of N_2 gas with a flow rate of 60 mL/min and a partially

reactive one with 110 mL/min steam supplied to the furnace together with 20 mL/min of protective N_2 gases. The relative humidity of supplied steam was set to 50% at a 50 °C temperature. Thus, thermal stability and other important properties of the feedstocks were revealed by applying selected conditions of thermochemical conversion on a small scale using thermogravimetry prior to analysis in the reactor.

The thermochemical conversion experiments described below were implemented by referring to the scientific research on the steam gasification of plastic wastes in a fluidized bed reactor [22,23].

2.3. Fluidized Bed Reactor System

The gasification experiments were carried out in a 1.3 m height stainless steel tube reactor with an inner diameter of approximately 8 cm. Other vital parts of the bubbling fluidized bed reactor were the reactor oven, the inlet system of fluidization gases, and the collection and processing system of produced gas flow. The internal setup of the reactor is shown in Figure 2.

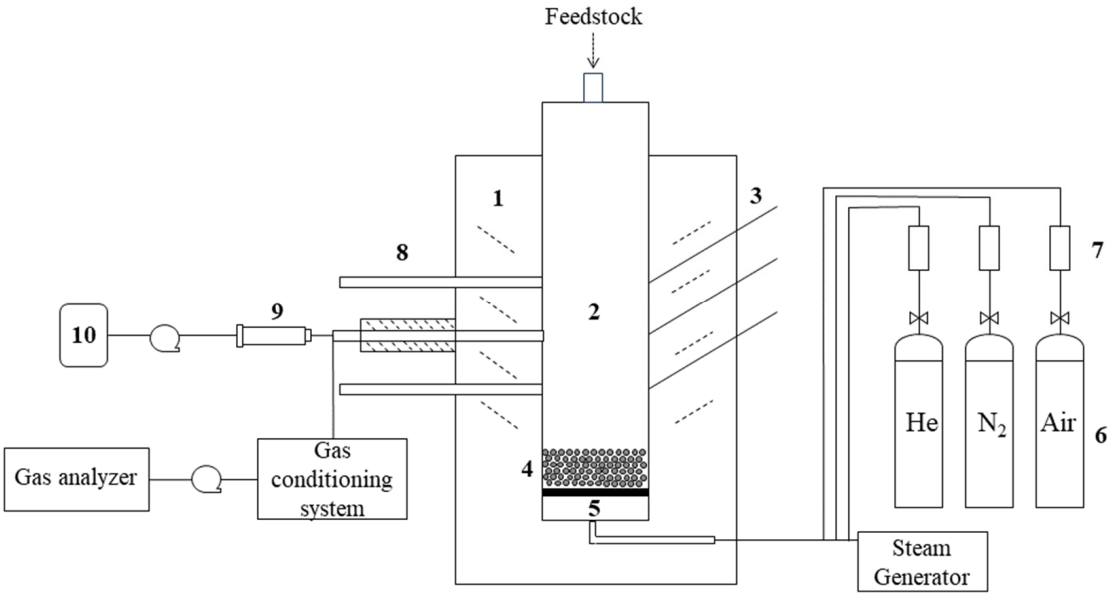

Figure 2. Bubbling fluidized bed reactor system employed for the steam gasification experiments: 1—reactor oven, 2—reactor, 3—thermocouples, 4—fluidized bed, 5—windbox, 6—gas balloons, 7—mass flow controllers, 8—sampling probes, 9—SPE amine, 10—Tedlar gas bag.

The tube reactor was electrically heated to reach the selected temperature values for the thermochemical conversion of the feedstock. Different thermocouples are installed inside the reactor to continuously measure and log the temperature along the height of the tube. The temperature of the fluidized bed is measured by the thermocouple located at the bottom of the reactor, as seen in Figure 2. The other thermocouples are used to control the temperature in the freeboard, which was set to the same temperature point as in the bed. The temperature of the fluidized bed is considered the reaction temperature. To develop the fluidization state, nitrogen and steam, acting as fluidization gases, were introduced from the bottom of the reactor. These gases were premixed in a windbox before entering the reactor through a gas distributor plate. For gasification, steam (superheated) was supplied at different flow rates, as presented in Table 1, through a windbox heated to the same temperature as set in the bed. To regulate the volumetric flow rate of the used fluidization gases, mass flow controllers (MFC) were used.

Table 1. Composition of supplied gases and steam flows during the pyrolysis/gasification and combustion process stages.

SCR	Steam (g/min)	N_2 (L/min)	He (L/min)	Air (L/min)
0	0	5	0.05	0
1	1.63	3	0.05	0
2	3.26	2	0.05	0
Combustion	0	0	0.05	5

The channels located on the side of the reactor (Figure 2) serve as the sampling probes required for sampling the evolved gases. The thermo-isolated sampling probe located approximately 32 cm height from the bottom of the reactor was used to sample the gases produced while the other probes were sealed to prevent bed material and generated products from exiting the reactor. The employed sampling port was heated up to 350 °C to avoid the condensation of released compounds of higher molecular weight and steam.

For the sampling of the gas, the gas stream is split into two streams, with one stream passing through a gas conditioning system and the other passing through an amine used for solid-phase extraction (SPE). The gas conditioner consists of scrubbing and cooling the sampled gas with isopropanol, then drying the gas with silica gel beads and glass wool. The dry, cold gas is then analyzed using a SICK GMS 820 (equipment sourced from Waldkrirch, Germany) permanent gas analyzer. The second gas stream goes to the SPE amine Supelclean TM Envi-CarbTM/NH_2 tube, obtained from Sigma-Aldrich (equipment sourced from Schnelldorf, Germany). The gas samples were collected in 0.5 L Tedlar gas bags and were analyzed in an Agilent 490 Micro gas chromatography system (equipment sourced from Waldbronn, Germany) to measure the composition.

2.4. Gasification Process Conditions

Different conditions were selected to evaluate the impact of the conversion temperature and the ratio of steam to carbon content in a fuel applied during the process. Two reaction temperatures, i.e., 700 °C and 800 °C, and three different ratio values of steam to carbon (SCR) content in feedstock (i.e., 0, 1, and 2) were tested in accordance with previous investigations [22,23].

Experiments were carried out using a batch feeding method adding around 2 g (±0.25 g) of a sample to the heated fluidized bed reactor from the top of the reactor. For all experiments, silica sand composed of 99.20% of SiO_2, 0.17% of Al_2O_3, and 0.05% of Fe_2O_3 in mass percentage was used as the bed material (component 4 in Figure 2), which was also inserted from the top of the reactor before implementing the experiments. The minimum value of fluidization velocity for the experiments was equal to 0.05 m/s. The average density of the silica sand particles was 2650 kg/m^3, and the average diameter of the particles was 316 µm.

As previously explained, the process was divided into two stages—firstly, the pyrolysis/gasification of the raw material was performed, and then the combustion of the formed char was accomplished by switching the fluidization gases supplied to the reactor. For this purpose, the steam was switched off to avoid further char gasification, and nitrogen was switched to air. The composition of the fluidization gases and the different steam flows are provided in Table 1.

The thermochemical conversion process step took 120 s, and the combustion step for the formed char was 60 s. The duration of gasification/pyrolysis and combustion stages were selected according to the evolved gases—products were continuously monitored with a gas analyzer to determine the time required for the conversion of separate feedstocks.

In both stages, gases released were collected, and the composition was analyzed as described in Sections 2.5 and 2.6. The analysis of gaseous products in the second stage of the process was to calculate the char content formed according to the carbon mass balance.

2.5. Composition of Evolved Gases Analysis

The micro gas chromatography (μGC) approach was employed for the detection of main gaseous products and the determination of their concentrations. Gaseous species analyzed by a μGC instrument included H_2, CO, CO_2, CH_4, C_2H_4, C_2H_6, C_2H_2, C_3H_x, C_4H_x, and N_2. Gaseous compounds containing three and four carbon atoms were analyzed as C_3H_x and C_4H_x because the μGC was not calibrated for different species separation of these hydrocarbons; therefore, the total area of the peaks in the chromatograms corresponded to the total amounts of the C3 and C4 species. Inert gases of helium and argon were used as a mobile phase, and two chromatography columns were present in the μGC to separate the compounds—Poraplot Q and MS5Å. The instrument was programmed to inject gases from Tedlar bags every 3 min with the cleaning step between different samples with the air alone.

2.6. Composition of Tars Analysis

The solid-phase adsorption (SPA) method [23,24] was employed to collect condensable aromatic hydrocarbons from the stream of volatile products formed during steam gasification. In this method, a low quantity of raw gas flows through an amine-carrying syringe that retains tars. Absorbed hydrocarbons were eluted afterward and analyzed using Bruker GC-FID equipment. The temperature ramp from 50 to 350 °C was applied to evaluate the composition of tars, including both monocyclic and polycyclic aromatic hydrocarbons. The split ratio used was equal to 20, and helium of 1 mL/min was employed as a mobile phase in the chromatography measurement. Three repetitions of every vial analysis were performed to obtain the mean abundance values of the compounds detected.

2.7. Evaluation of Carbon Content in Products

To evaluate the carbon content in three different phases of products, calculations based on [23] were accomplished. Using this approach, the char amount accumulated from each sample during the gasification was also evaluated. Performing the combustion stage, the gases formed were collected, and concentrations (%) of char combustion products (CO and CO_2) were measured using μGC. These data were then converted to molar yields per feedstock kilogram by employing the He-tracing method, where the equation is presented below (Equation (1)). Helium was chosen as a tracer gas—since the reaction with other compounds does not exist, the inert gas He passes the system without changing. Therefore, the variations of trace gas concentration in the products stream can be considered as changes in yields of produced gases.

$$n_i = \frac{c_i}{m_f} \times \left(\frac{V_{He-tracing}}{C_{He}} \right) \times \frac{1}{V_m} \quad (1)$$

In Equation (1), n_i is the molar yield of gases produced (mol/kg), c_i is the concentration of gaseous species in percentage (%) determined using μGC, m_f—the weight of a feed (kg), $V_{He\text{-}tracing}$—volume of He supplied (**L**), C_{He}—concentration of He (%) measured by μGC, and V_m—is the molar volume of an ideal gas at 25 °C temperature.

3. Results and Discussion

3.1. Thermogravimetric Analysis

In order to determine thermal decomposition points together with mass changes of 3PFM and KN95 face masks upon heating, thermogravimetric analysis in the ambient of N_2 gas and steam was carried out. The obtained thermogravimetric (TG) and differential thermogravimetric (DTG) curves are presented in Figure 3.

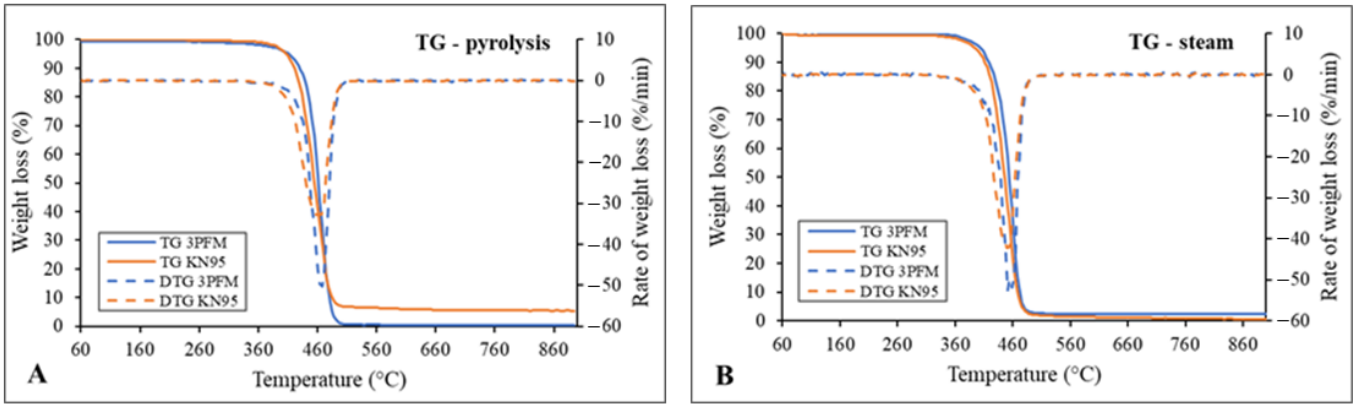

Figure 3. Weight loss (%) and thermal degradation rate (%/min) curves obtained by heating feedstocks in the inert ambient of nitrogen (**A**) and partially reactive ambient with steam (**B**).

TG analysis curves revealed that the thermal degradation of both feedstocks occurs in a single stage that corresponds to the devolatilization of feedstocks, during which >95 wt.% of the volatile matter is released due to intense breakage of the chemical bonds present in the polymer with the absence of solid carbon formation. The reason for such a degradation pathway is determined by the structure of the polymer comprising the feedstock, polypropylene, which has a liner structure [25]. Thus, the formation of char is expected to be minor. The onset temperature of decomposition was estimated to vary insignificantly depending on the inertness of the ambient—both samples of protective masks started to decompose at 310 ± 2 °C temperature and degraded completely at a temperature of up to 516 ± 2 °C. Temperature points at which the weight loss rate (DTG) was the highest were also closely similar when comparing both feedstocks, i.e., it was equal to 467 ± 1 °C in inert and 450 °C in the ambient with steam. Similar results were obtained by A. Nawaz & P. Kumar [26], who published that 3-ply protective face masks degradation onset was at higher than 300 °C temperature with the greatest decomposition rate at 456 °C when the applied heating rate during pyrolysis was 20 °C/min. These temperature points of thermal degradation are known to be specific to polypropylene [27]. The highest decomposition rate of the 3PFM sample was 50 ± 1%/min in both analyzed atmospheres, and that of the KN95 sample was 33%/min and 42.36%/min in the N_2 and steam ambient, respectively. Greater decomposition of the KN95 sample was a result of the oxidizing effect influenced by the presence of steam, which is also apparent by evaluating the TG curve. The residual mass of the KN95 was 5.46% after pyrolysis and reduced to 0.52% when the thermal analysis was completed in the steam ambient. Overall, TG analysis has revealed that 3PFM and KN95 face masks decompose at almost identical temperatures with the greatest decomposition rates at 467 ± 1 °C and 450 °C temperatures in the N_2 and steam ambient, respectively.

3.2. The Influence of Gasification Temperature on Gases Formation

In general terms, both feedstocks have comparable decomposition tendencies according to the gaseous species formation during pyrolysis/steam gasification processes. It is a consequence of the similar composition of both types of protective face masks. As mentioned before, the main polymer comprising both types of protective masks is polypropylene. D. Frączak et al. [28] have consistently described the mechanism of pyrolysis and gasification of polyolefins. During pyrolysis, a polymer's thermal cracking occurs, which is divided into the initiation, propagation, and termination steps. During the initiation, the branched parts break, and radicals are released when the C-H bond breaks. The second step is β-scission which results in different lengths of shorter hydrocarbon chain creation together with additional free radicals release. During the propagation step, secondary radicals form, and the isomerization of released lower molecular weight organic molecules occurs. In the last stage, secondary reactions between free radicals, such as recombination

and disproportionation, along with monocyclic and polycyclic hydrocarbons formation during cyclization and polycondensation, also affect char development. In contrast, the gasification process has a particularly different decomposition pattern due to the reactive ambient employed during the process. Similar to pyrolysis, polyolefin first undergoes the thermal cracking reactions described above, and then it is followed by reforming reactions that are determined by the oxidizing agent used in the process. The main steam reforming reactions that manage the generation of syngas are presented below in the text (reactions a and b).

It was detected that variations of selected gasification conditions significantly influenced the distribution of gaseous products. It was established that gasification temperature has a major influence on the distribution of gaseous species formed, whereas the SCR applied considerably impacted the concentration of syngas, CO_2, and some hydrocarbons evolved. The graphs presented in Figure 4 illustrate how the concentration of detected gases varied when different process conditions were employed.

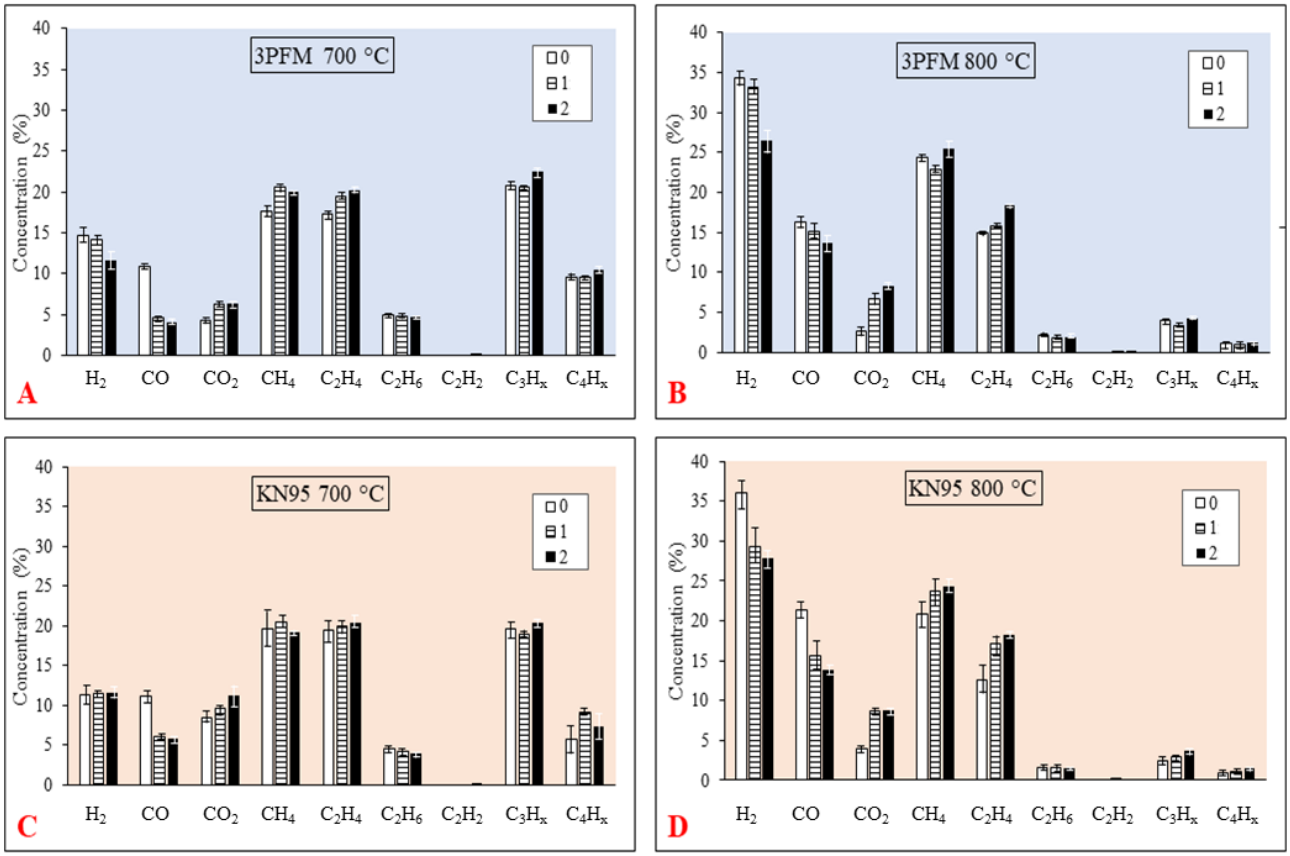

Figure 4. Distribution (%) of gaseous species formed during the steam gasification of 3PFM (**A**,**B**) and KN95 (**C**,**D**) face masks at 700 °C and 800 °C temperature by applying three different SCR values (0, 1, 2).

Since both feedstocks had similar decomposition tendencies during steam gasification, the influence of selected process conditions on gaseous product formation was compared, taking both feedstocks into account without distinguishing them. Generally, the process temperature had a crucial impact on the distribution of gaseous products formed from both feedstocks. Results of the μGC analysis of gases that evolved during the steam gasification of protective face mask pellets at 700 °C have revealed that the main gaseous products with a higher than 20% share were C_3H_x species. These mainly referred to propene [19] and propane since polypropylene undergoes carbon chain scission reactions under heating, followed by hydrogen relocation and donation [29]. Other gases with an important contribution were CH_4 and C_2H_4, which took around 20% for each at 700 °C

in all SCR cases, which is also influenced by the chemical reactions mentioned before. H_2 gases also evolved abundantly, with a share of around 15% at 700 °C. Contrastingly to the gasification temperature of 700 °C, at 800 °C, the main gaseous product formed was H_2, with the highest concentration of ~34%. On the contrary, the concentration of C_3H_x species declined considerably from <20% to ±4% with an increase in process temperature during the steam gasification of the protective face masks. This is explained by the greater cracking of a feedstock comprising polymer–polypropylene caused by higher temperatures applied during the process. Consequently, the formation of a lower molecular weight product, CH_4, was induced slightly at an 800 °C gasification temperature compared to 700 °C, whereas the C_2H_4 concentration at both temperatures remained almost unchanged. However, the CO share among gaseous products increased with the higher temperature applied, which was also considered to occur due to greater thermal decomposition of a feedstock. V. Wilk & H. Hofbauer [30] have also found that the main gases that form during the steam gasification of polypropylene plastic wastes are hydrocarbons of low molecular weight (up to C4) at a gasification temperature of 640 °C and the increase of process temperature to 850 °C induced the formation of H_2 making it the second most abundant product of less than 35% concentration with the highest abundance of CH_4 with a share of ~40%. C. Wu & P. T. Williams [31] revealed that gasification temperature influences the formation of H_2 gases during steam gasification of pure PP–hydrogen gases, which is the main product with a 52% concentration at 900 °C temperature. Together with H_2 gas, the evolution of CO was also induced by process temperature increments [32]. Therefore, high process temperature is fundamental for syngas generation from PP-rich wastes.

3.3. The Influence of Steam to Carbon Ratio on Gases Formation

The amount of oxidizing agent (steam to carbon ratio applied) along with the process temperature significantly influenced the composition of gases during the steam gasification of 3PFM and KN95 face masks. It was determined that the increment of applied SCR has almost no impact on syngas (g/kg) formation at both temperatures of thermochemical conversion. The weight yields of H_2 and CO per kilogram of feedstock produced are presented in Figure 5.

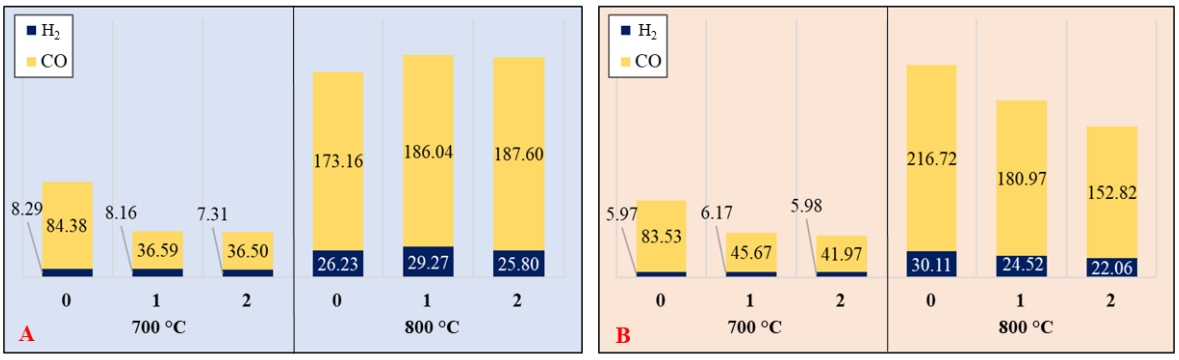

Figure 5. Yields (g/kg fuel) of syngas produced from 3PFM (**A**) and KN95 face masks (**B**) using steam gasification (SCR = 0; 1; 2).

Obtained results (Figure 5) reveal that hydrogen production from 3PFM compared with KN95 was greater in most cases. The influence of process temperature was distinguished as a major factor influencing the composition of product gas. Higher temperatures induced the formation of syngas from both feedstocks, although the influence of SCR on H_2 gas formation was smaller. At both temperatures studied, a negligible reduction of H_2 production was determined. A similar trend was observed comparing the yields of CO gas. Therefore, in contrast to the elevation of temperature, increasing the value of SCR had a negative effect on the amount of syngas produced. S. Li et al. [22] have established similar trends of syngas formation from polyethylene terephthalate (PET) during steam gasification in a bubbling fluidized bed. The evolution of H_2 was induced only slightly, while

CO formation was diminished with the SCR rise from 1.25 to 3.75, which was explained by the water gas shift reaction (b) introduced below. Contrastingly, A. Erkiaga et al. [33] revealed that the syngas (% vol.) formation from HDPE was induced by >50% when the steam/plastic ratio was increased from 0 to 2 during steam gasification at 900 °C, although the important factor is the use of a catalyst (olivine and γ-Al_2O_3), which was employed during the process. According to previously conducted research on the steam gasification of different wastes [19,32,34–38], in most cases, it was reported that a catalyst is required for the steam reforming reaction (2) to occur. Thus, the presence of reaction (2) was unlikely during the gasification experiments in this investigation since the formation of syngas was not significantly induced with a higher amount of steam supplied.

$$C_nH_m + nH_2O \leftrightarrow \left(\frac{m}{2} + n\right)H_2 + nCO \quad (2)$$

$$CO + H_2O \rightarrow CO_2 + H_2 \quad (3)$$

Increasing the SCR was estimated to greatly influence low molecular weight hydrocarbon development (Figure 4), especially methane, ethene, and C3 and C4 species. The higher amount of oxidizing agent, which was steam in our case, along with higher temperatures, triggers thermal cracking of the tars formed after breakage of a feedstock comprising polymer—mainly polypropylene. Thus, it was also a consequence of decreased syngas (%) evolution detected with μGC since it was diluted with light hydrocarbons together with CO_2 gas, where the concentration was also boosted owing to the oxidation of hydrocarbons when the steam supply was improved. It is also considered that the water gas shift reaction (b) had resulted in the induced CO_2 formation, although to a smaller extent, since the formation of hydrogen, as discussed before, was not improved. On the contrary, S. Li et al. [22] reported that during PET steam gasification, hydrogen production was induced slightly with the elevation of the steam-to-fuel ratio from 1.25 to 3.75, although the formation of CO, CO_2, and C2 and C3 species concentration declined in the products stream. Compared to our obtained results in this research, this difference was present due to the used bed material olivine, which has reforming activity [39], i.e., it catalyzes the chemical reaction (a) during the conversion process.

3.4. The Influence of Gasification Conditions on the Composition of Tars

Figure 6 illustrates the changes in yields of aromatic hydrocarbons formed during the gasification. The main compounds determined using the GC-FID approach were benzene, toluene, and naphthalene in all cases. The formation of monoaromatic and diaromatic compounds during steam gasification of polypropylene-produced face masks is a consequence of the Diels–Alder reaction. During the thermal decomposition of the present polymer, C3 and C4 species evolved in abundance (Figure 4), which mainly corresponded to olefins that are known to be reactive and form benzene rings through referred reaction [40], which is also the reason for the increased H_2 gases production due to dehydrogenation.

The distribution pattern of aromatic compounds resembled both types of face masks under the same gasification conditions. Generally, the formation of tars (Figure 6) was induced by higher gasification temperature together with greater SCR applied both from 3PFM and KN95 masks. That is, the influence of the intense decomposition of both feedstocks resulted in the greater evolution of low molecular weight gases such as propene and butene, which are the initial compounds for the generation of aromatic hydrocarbons. Therefore, both temperature elevation and a higher ratio of steam to carbon have induced benzene formation due to greater decomposition of the primary material of both feedstocks. Contrary to that, S. Li et al. [22] have shown that the formation of aromatic hydrocarbons from PET decreased with the gasification temperature elevation together with the increase in SCR. This can be accepted as a consequence of the catalytic activity of the bed material (olivine) to greater cracking of tars generated during steam gasification.

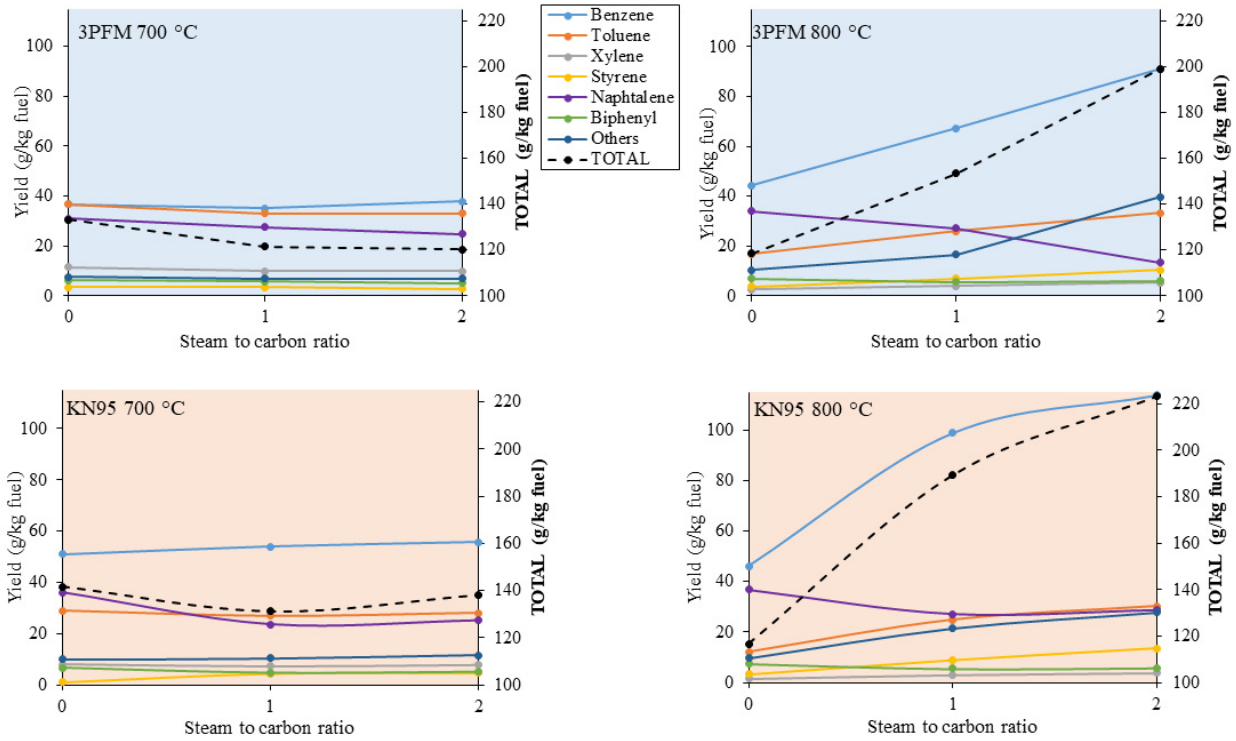

Figure 6. Composition of the tars determined with different temperatures and steam-to-carbon ratios applied during the steam gasification of 3PFM and KN95 face masks.

3.5. Product Yields—Conversion Efficiency

A carbon conversion rate was calculated to evaluate the conversion process efficiency, which represents the amount (%) of total carbon in the feedstock converted to gaseous products. The accumulation of solid carbon during the thermochemical conversion of feedstock was evaluated as described in Section 2.5. The estimated values of carbon atoms quantity distribution among three separate product phases are illustrated in Figure 7. The amount of carbon converted to tars is presented together with the species of C5 and C6 aliphatic hydrocarbons that were outside the scope of the µGC analysis employed in this research.

Figure 7. Carbon (%) distribution in the gas, tars, and char phases originated from the 3PFM (**A**) and KN95 (**B**) face mask steam gasification (y-axis corresponds to the SCR_temperature of the process).

The greatest carbon conversion to gaseous products was achieved at 800 °C with an SCR value of 2 for the 3PFM feedstock, which was equal to 92.7%. The high conversion rates were caused by higher hydrocarbon cracking when a greater portion of the oxidizing agent

was supplied at a high conversion temperature. Meanwhile, that of the KN95 feedstock was only 78.06% at 800 °C with an SCR equal to 1. Thus, it was generally determined that the 3PFM feedstock was converted to gaseous products to a greater extent than the KN95 feedstock at the same thermochemical conversion conditions. Additionally, it was estimated that the carbonization of the KN95 was higher than 3PFM during the conversion process. Overall, the carbonization proceeded most intensely during the pyrolysis (SCR = 0) at a process temperature of 800 °C, together with the lowest rates of gases produced.

Overall, the analysis results of evolved gas composition and yields revealed that the influence of temperature during the thermochemical conversion process of facial masks plays a vital role in value-added gaseous product synthesis. This is explained by several well-established factors. The higher temperature applied influences the production of gas in higher yields, i.e., the bed material is heated to a greater extent, more energy is transmitted, and initial cracking is boosted. Along with primary cracking, the secondary cracking of hydrocarbons improved, resulting in improved formation of lower molecular weight gas. From these statements, it is implied that higher temperatures (above 800 °C) for non-catalytic thermochemical conversion have great potential for further studies of plastic waste conversion using pyrolysis and gasification and for implementing these processes more widely in the future.

4. Conclusions

Valorization of 3-ply face masks and KN95 respirator wastes through pyrolysis/steam gasification by employing a fluidized bed reactor was investigated in this research. It was determined that the temperature and amount of steam supplied to the reactor influenced the distribution of evolved gaseous products significantly. The composition of gases formed from 3-ply face masks and KN95 respirators by applying the respective parameters were detected to be nearly equivalent. In both cases, the main gases produced were light hydrocarbons such as species of C_3H_x, CH_4, and C_2H_4 at the conversion temperature of 700 °C. While higher temperatures (i.e., 800 °C) influenced greater decomposition of volatile matter of both feedstocks, the formation of H_2 occurred to a greater extent. It was revealed that the steam under non-catalytic conditions of gasification has no or low influence on syngas formation; only a slight positive effect was present when the steam-to-carbon ratio applied was equal to 1 during steam gasification of 3-ply face masks. The experimental findings presented in this work show that disposable protective face masks can be chemically recycled into syngas using pyrolysis/steam gasification at $\geq$800 °C temperature escaping the need for catalyst employment during the conversion process.

Author Contributions: Conceptualization, I.K., N.S., J.E. and M.S.; Methodology, I.K., J.G.-A. and J.E.; Validation, N.S. and M.S.; Formal analysis, I.K., J.G.-A., N.S., J.E. and M.S.; Investigation, I.K.; Resources, J.E.; Data curation, J.G.-A., N.S. and M.S.; Writing—original draft, I.K.; Writing—review & editing, I.K. and J.G.-A.; Visualization, I.K.; Supervision, J.G.-A., N.S., J.E. and M.S. All authors have read and agreed to the published version of the manuscript.

Funding: This research was funded by European Regional Development Fund (project No 13.1.1-LMT-K-718-05-0017) under grant agreement with the Research Council of Lithuania (LMTLT). Funded as European Union's measure in response to Cov-19 pandemic.

Data Availability Statement: Data sharing not applicable. No new data were created or analyzed in this study. Data sharing is not applicable to this article.

Acknowledgments: The visit to the partners (Chalmers University of Technology) where experimental data was collected was financed as a part of the Nordic Energy Research Programme (NERP) project Establishment of Nordic-Baltic and researcher mobility network in the field of bioenergy (REMONET-Bioenergy). Authors express their great gratitude to Chahat Mandviwala for all the engineering solutions implemented on analysis instruments and help provided through revision process of manuscript.

Conflicts of Interest: The authors declare no conflict of interest.

References

1. WHO. Coronavirus Disease (COVID-19) Pandemic—Overview. Available online: https://www.who.int/europe/emergencies/situations/covid-19 (accessed on 6 December 2022).
2. Mofijur, M.; Fattah, I.M.R.; Alam, M.A.; Islam, A.B.M.S.; Ong, H.C.; Rahman, S.M.A.; Najafi, G.; Ahmed, S.F.; Uddin, A.; Mahlia, T.M.I. Impact of COVID-19 on the Social, Economic, Environmental and Energy Domains: Lessons Learnt from a Global Pandemic. *Sustain. Prod. Consum.* **2021**, *26*, 343–359. [CrossRef] [PubMed]
3. WHO. Coronavirus Disease (COVID-19): How Is It Transmitted? Available online: https://www.who.int/news-room/questions-and-answers/item/coronavirus-disease-covid-19-how-is-it-transmitted#:~:text=The%20virus%20can%20spread%20from,%2C%20speak%2C%20sing%20or%20breathe (accessed on 7 December 2022).
4. Peng, Y.; Wu, P.; Schartup, A.T.; Zhang, Y. Plastic Waste Release Caused by COVID-19 and Its Fate in the Global Ocean. *Proc. Natl. Acad. Sci. USA* **2021**, *118*, e2111530118. [CrossRef]
5. WHO. Tonnes of COVID-19 Health Care Waste Expose Urgent Need to Improve Waste Management Systems. Available online: https://www.who.int/news/item/01-02-2022-tonnes-of-covid-19-health-care-waste-expose-urgent-need-to-improve-waste-management-systems#:~:text=Tens%20of%20thousands%20of%20tonnes,to%20a%20new%20WHO%20report (accessed on 9 December 2022).
6. McCarthy, R.; Gino, B.; d'Entremont, P.; Barari, A.; Renouf, T.S. The Importance of Personal Protective Equipment Design and Donning and Doffing Technique in Mitigating Infectious Disease Spread: A Technical Report. *Cureus* **2020**, *12*, e12084. [CrossRef]
7. Jiangtao, S.; Zheng, W. Coronavirus: China Struggling to Deal with Mountain of Medical Waste Created by Epidemic. Available online: https://www.scmp.com/news/china/society/article/3065049/coronavirus-china-struggling-deal-mountain-medical-waste-created (accessed on 20 December 2022).
8. Yang, S.; Cheng, Y.; Liu, T.; Huang, S.; Yin, L.; Pu, Y.; Liang, G. Impact of Waste of COVID-19 Protective Equipment on the Environment, Animals and Human Health: A Review. *Environ. Chem. Lett.* **2022**, *20*, 2951–2970. [CrossRef]
9. Spennemann, D.H.R. COVID-19 Face Masks as a Long-Term Source of Microplastics in Recycled Urban Green Waste. *Sustainability* **2021**, *14*, 207. [CrossRef]
10. Akkajit, P.; Romin, H.; Assawadithalerd, M.; Al-Khatib, I.A. Assessment of Knowledge, Attitude, and Practice in Respect of Medical Waste Management among Healthcare Workers in Clinics. *J. Environ. Public Health* **2020**, *2020*, 8745472. [CrossRef]
11. Jung, S.; Lee, S.; Dou, X.; Kwon, E.E. Valorization of Disposable COVID-19 Mask through the Thermo-Chemical Process. *Chem. Eng. J.* **2021**, *405*, 126658. [CrossRef] [PubMed]
12. Verma, R.; Vinoda, K.S.; Papireddy, M.; Gowda, A.N.S. Toxic Pollutants from Plastic Waste—A Review. *Procedia Environ. Sci.* **2016**, *35*, 701–708. [CrossRef]
13. Purnomo, C.W.; Kurniawan, W.; Aziz, M. Technological Review on Thermochemical Conversion of COVID-19-Related Medical Wastes. *Resour. Conserv. Recycl.* **2021**, *167*, 105429. [CrossRef]
14. Safdari, M.-S.; Amini, E.; Weise, D.R.; Fletcher, T.H. Heating Rate and Temperature Effects on Pyrolysis Products from Live Wildland Fuels. *Fuel* **2019**, *242*, 295–304. [CrossRef]
15. Greco, G.; Videgain, M.; Di Stasi, C.; Pires, E.; Manyà, J.J. Importance of Pyrolysis Temperature and Pressure in the Concentration of Polycyclic Aromatic Hydrocarbons in Wood Waste-Derived Biochars. *J. Anal. Appl. Pyrolysis* **2021**, *159*, 105337. [CrossRef]
16. Miandad, R.; Barakat, M.A.; Aburiazaiza, A.S.; Rehan, M.; Nizami, A.S. Catalytic Pyrolysis of Plastic Waste: A Review. *Process Saf. Environ. Prot.* **2016**, *102*, 822–838. [CrossRef]
17. Anekwe, I.M.S.; Khotseng, L.; Isa, Y.M. The Place of Biofuel in Sustainable Living; Prospects and Challenges. In *Comprehensive Renewable Energy*; Elsevier: Amsterdam, The Netherlands, 2022; pp. 226–258.
18. Farooq, A.; Lee, J.; Song, H.; Ko, C.H.; Lee, I.-H.; Kim, Y.-M.; Rhee, G.H.; Pyo, S.; Park, Y.-K. Valorization of Hazardous COVID-19 Mask Waste While Minimizing Hazardous Byproducts Using Catalytic Gasification. *J. Hazard. Mater.* **2022**, *423*, 127222. [CrossRef] [PubMed]
19. Nam, J.Y.; Lee, T.R.; Tokmurzin, D.; Park, S.J.; Ra, H.W.; Yoon, S.J.; Mun, T.-Y.; Yoon, S.M.; Moon, J.H.; Lee, J.G.; et al. Hydrogen-Rich Gas Production from Disposable COVID-19 Mask by Steam Gasification. *Fuel* **2023**, *331*, 125720. [CrossRef] [PubMed]
20. Oyeleke, O.O.; Ohunakin, O.S.; Adelekan, D.S. Catalytic Pyrolysis in Waste to Energy Recovery Applications: A Review. *IOP Conf. Ser. Mater. Sci. Eng.* **2021**, *1107*, 012226. [CrossRef]
21. Yung, M.M.; Starace, A.K.; Griffin, M.B.; Wells, J.D.; Patalano, R.E.; Smith, K.R.; Schaidle, J.A. Restoring ZSM-5 Performance for Catalytic Fast Pyrolysis of Biomass: Effect of Regeneration Temperature. *Catal. Today* **2019**, *323*, 76–85. [CrossRef]
22. Li, S.; Cañete Vela, I.; Järvinen, M.; Seemann, M. Polyethylene Terephthalate (PET) Recycling via Steam Gasification—The Effect of Operating Conditions on Gas and Tar Composition. *Waste Manag.* **2021**, *130*, 117–126. [CrossRef]
23. Mandviwala, C.; Berdugo Vilches, T.; Seemann, M.; Faust, R.; Thunman, H. Thermochemical Conversion of Polyethylene in a Fluidized Bed: Impact of Transition Metal-Induced Oxygen Transport on Product Distribution. *J. Anal. Appl. Pyrolysis* **2022**, *163*, 105476. [CrossRef]
24. Israelsson, M.; Seemann, M.; Thunman, H. Assessment of the Solid-Phase Adsorption Method for Sampling Biomass-Derived Tar in Industrial Environments. *Energy Fuels* **2013**, *27*, 7569–7578. [CrossRef]
25. Park, S.-J.; Seo, M.-K. Element and Processing. In *Interface Science and Technology*; Elsevier: Oxford, UK, 2011; pp. 431–499.

26. Nawaz, A.; Kumar, P. Thermal Degradation of Hazardous 3-Layered COVID-19 Face Mask through Pyrolysis: Kinetic, Thermodynamic, Prediction Modelling Using ANN and Volatile Product Characterization. *J. Taiwan Inst. Chem. Eng.* **2022**, *139*, 104538. [CrossRef]
27. Esmizadeh, E.; Tzoganakis, C.; Mekonnen, T.H. Degradation Behavior of Polypropylene during Reprocessing and Its Biocomposites: Thermal and Oxidative Degradation Kinetics. *Polymers* **2020**, *12*, 1627. [CrossRef] [PubMed]
28. Frączak, D. Chemical Recycling of Polyolefins (PE, PP): Modern Technologies and Products. In *Waste Material Recycling in the Circular Economy—Challenges and Developments*; IntechOpen: London, UK, 2022.
29. Damayanti, D.; Saputri, D.R.; Marpaung, D.S.S.; Yusupandi, F.; Sanjaya, A.; Simbolon, Y.M.; Asmarani, W.; Ulfa, M.; Wu, H.S. Current Prospects for Plastic Waste Treatment. *Polymers* **2022**, *14*, 3133. [CrossRef] [PubMed]
30. Wilk, V.; Hofbauer, H. Conversion of Mixed Plastic Wastes in a Dual Fluidized Bed Steam Gasifier. *Fuel* **2013**, *107*, 787–799. [CrossRef]
31. Wu, C.; Williams, P.T. Effects of Gasification Temperature and Catalyst Ratio on Hydrogen Production from Catalytic Steam Pyrolysis-Gasification of Polypropylene. *Energy Fuels* **2008**, *22*, 4125–4132. [CrossRef]
32. Wu, C.; Williams, P.T. Hydrogen Production by Steam Gasification of Polypropylene with Various Nickel Catalysts. *Appl. Catal. B* **2009**, *87*, 152–161. [CrossRef]
33. Erkiaga, A.; Lopez, G.; Amutio, M.; Bilbao, J.; Olazar, M. Syngas from Steam Gasification of Polyethylene in a Conical Spouted Bed Reactor. *Fuel* **2013**, *109*, 461–469. [CrossRef]
34. Lazzarotto, I.P.; Ferreira, S.D.; Junges, J.; Bassanesi, G.R.; Manera, C.; Perondi, D.; Godinho, M. The Role of CaO in the Steam Gasification of Plastic Wastes Recovered from the Municipal Solid Waste in a Fluidized Bed Reactor. *Process Saf. Environ. Prot.* **2020**, *140*, 60–67. [CrossRef]
35. Zhou, C.; Stuermer, T.; Gunarathne, R.; Yang, W.; Blasiak, W. Effect of Calcium Oxide on High-Temperature Steam Gasification of Municipal Solid Waste. *Fuel* **2014**, *122*, 36–46. [CrossRef]
36. Jeong, Y.-S.; Park, K.-B.; Kim, J.-S. Hydrogen Production from Steam Gasification of Polyethylene Using a Two-Stage Gasifier and Active Carbon. *Appl. Energy* **2020**, *262*, 114495. [CrossRef]
37. Wang, J.; Cheng, G.; You, Y.; Xiao, B.; Liu, S.; He, P.; Guo, D.; Guo, X.; Zhang, G. Hydrogen-Rich Gas Production by Steam Gasification of Municipal Solid Waste (MSW) Using NiO Supported on Modified Dolomite. *Int. J. Hydrogen Energy* **2012**, *37*, 6503–6510. [CrossRef]
38. Han, S.W.; Tokmurzin, D.; Lee, J.J.; Park, S.J.; Ra, H.W.; Yoon, S.J.; Mun, T.-Y.; Yoon, S.M.; Moon, J.H.; Lee, J.G.; et al. Gasification Characteristics of Waste Plastics (SRF) in a Bubbling Fluidized Bed: Use of Activated Carbon and Olivine for Tar Removal and the Effect of Steam/Carbon Ratio. *Fuel* **2022**, *314*, 123102. [CrossRef]
39. Kuhn, J.N.; Zhao, Z.; Felix, L.G.; Slimane, R.B.; Choi, C.W.; Ozkan, U.S. Olivine Catalysts for Methane- and Tar-Steam Reforming. *Appl. Catal. B* **2008**, *81*, 14–26. [CrossRef]
40. Park, K.-B.; Jeong, Y.-S.; Kim, J.-S. Activator-Assisted Pyrolysis of Polypropylene. *Appl. Energy* **2019**, *253*, 113558. [CrossRef]